

CHAPTER 3

RESEARCH SCOPE AND INITIAL STUDY

3.1 Introduction

Based on the field measurements and previous researches, it is found that the following factors may usually control the effects of high horizontal stress on entry roof stability:

- (1) the geological and mining conditions;
- (2) the angle between the orientation of horizontal stress and mining direction;
- (3) the ratios of the maximum to minimum horizontal stresses ($\sigma_{h \max} / \sigma_{h \min}$);
- (4) the magnitude of the horizontal stress;
- (5) the sequence of cutting and mining in entry development;
- (6) the properties in the interfaces between the coal seam and the roof/floor and between the roof layers (laminated roof).

In the study, the influence of these factors on the stress distributions in the immediate roof of longwall entries will be analyzed.

3.2 Research Scope

3.2.1 Geological and Mining Conditions

It is found that roof failure often occurs where the immediate roof consists of laminated/bedded shale or similar weak rock, as shown in Table 3-1. This study has been based on the typical geological and mining conditions of the Pittsburgh coal seam. The typical immediate roof consists of laminated/bedded thinly shale. Since the strength of shale changes locally, two types of shale will be considered in the study, namely weak shale and medium strength shale as shown in Fig. 3-1. In this study, the properties of coal and floor rock are kept the same.

As shown in Tables 2-1, 2-2, and 3-1, the overburden depth where roof failures occur is under 1,500 ft, mainly between 600 ft and 1,200 ft. Therefore, the overburden depths in the initial study will be 500 ft, 800 ft and 1,300 ft. The mining height is 7 ft and

Thick-ness (ft)	Log (not scale)	Rock Type	Young's Modulus (x10 ⁶ psi)	Poisson's Ratio	Compre. Strength (psi)	Cohesion (psi)	Friction Angle (°)
42		Siltstone	2.1	0.21	6,500	1,350	25
		shale	1.5	0.22	5,500	1,200	28
		shalewith sandstone	1.68	0.22	5,200	1,630	30
8		Weak shale	0.55	0.25	3,500	1,000	32
7		Coal	0.35	0.30	1,200	900	35
5		Shale	1.5	0.22	5,500	1,200	26
45		Claystone	1.1	0.3	1,300	760	35
		Shale with sandstone	1.68	0.22	5,200	1,630	30

(a) Weak Roof

Thick-ness (ft)	Log (not scale)	Rock Type	Young's Modulus (x10 ⁶ psi)	Poisson's Ratio	Compre. Strength (psi)	Cohesion (psi)	Friction Angle (°)
42		Siltstone	2.1	0.21	6,500	1,350	25
		shale	1.5	0.22	5,500	1,200	28
		shalewith sandstone	1.68	0.22	5,200	1,630	30
8		Shale	1.5	0.22	5,500	1,200	28
7		Coal	0.35	0.30	1,200	900	35
5		Shale	1.5	0.22	5,500	1,200	26
45		Claystone	1.1	0.3	1,300	760	35
		Shale with sandstone	1.68	0.22	5,200	1,630	30

(a) Medium Roof

Fig. 3-1 The Geological Conditions Used in the Models
(the data from Su^[39] and our lab test data)

the longwall face is 800 ft wide. The entry width is 18 ft and 3-entry development system has been mainly considered in the finite element modeling.

3.2.2 Influence of Stress Angle on Stability of Entry Roof

The field measurements have confirmed that the angle between the orientation of maximum horizontal stress and the mining (or entry development) direction has a very significant effect on the roof stability in longwall entry systems^[23, 39]. In the initial study, the angles, 15⁰, 30⁰, 45⁰, 60⁰, 75⁰, and 90⁰, are taken into account. After the initial study, the angle range, in which the angle has a significant effect on the stress distribution in the entry roof, will be determined. Then, in this range, the angle influence on entry roof will be analyzed in three situations: entry development period, single panel mining, and multiple panel mining. For the multiple panel system, the maximum horizontal stress comes either from the solid coal side or from the mined-out (gob) side.

During an entry development, underground observations have confirmed that cutter roof failures occurred in different places. What causes this? In this study, it attempts to find if there are some relations between the cutter roof failure and the angle between the orientation of maximum horizontal stress and the mining direction, namely, if the locations of cutter roof depend on the angle when all other conditions are fixed. The stress distributions around the entry system will be analyzed, especially the horizontal stress concentrations.

When a single panel is mining, how does the horizontal stress affect the stability of the headgate/tailgate entries? In this case, the gob will influence the entry systems. This effect may have some relation with the angle. As the angle changes, the effect will change. In this study, the roof stability in the T-junctions is the main concern.

In a multiple-panel system, since the previous panels are mined out and the current mining panel is adjacent to a gob on its one side, the entry systems of the current mining panel will be in different situations from those of the entry development and of the single panel. This is a complicated situation. At the seam level, the gob seems to separate the horizontal stress and makes the entries adjacent to the gob in the stress-relief zones. But, there exists a continuous deformation zone over the gob, which can be subjected to the horizontal stress. In this case, the horizontal stress will pass through the

gob and act on the chain pillars. If this situation is true, the entries adjacent to the gob will be in worse condition. In addition, the effects of the angle between the orientation of maximum horizontal stress and the mining direction on the entry roof in a multiple-panel system will be studied in detail.

3.2.3 Influence of Stress Ratio on Stability of Entry Roof

As shown in Tables 2-1 and 2-2, the horizontal stresses are biaxial, with a maximum horizontal stress much greater than the minimum horizontal stress. The ratio of maximum to minimum horizontal stresses ranges from 1.18 to 1.67 (Table 2-1) while it is about 1.23~1.68 in Table 2-2. In Table 2-1, the ratio of maximum horizontal to vertical stresses ranges from 4.3 to 7.4, while it is about 1.9~3.9 in Table 2. Up to now, the ratio effects on the roof stability have not been reported. If the ratio is smaller, the angle influence should not be significant. In this case, roof stability will be studied. Since this study is based on the Pittsburgh geological conditions, the overburden depths are 500 ft, 800 ft and 1,300 ft. So the vertical stress will be 550 psi, 880 psi and 1,430 psi, respectively in the finite element models. The ratios of maximum to minimum horizontal stresses will be:

$$\sigma_{hmax} / \sigma_{hmin} = 1.2, 1.5, \text{ and } 2.0$$

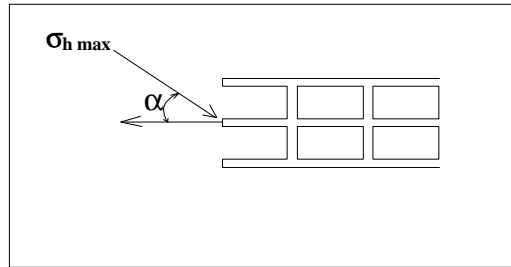
The maximum horizontal stresses (σ_{hmax}) will be 3,000 psi and 4,500 psi.

3.2.4 Sequence of Cutting and Mining in Entry Development

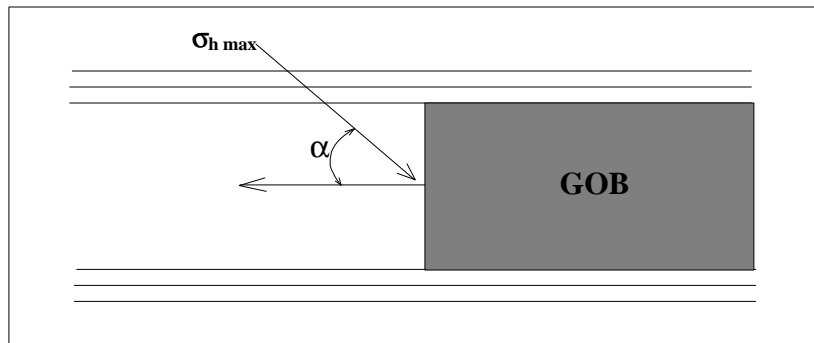
The sequence of cutting and mining in an entry development may affect the stress distributions in the immediate roof. In this study, this sequence will be simulated in a 3-entry system step by step, as shown in Fig. 3-3. In the same geological and stress conditions, the stress distributions will change with the different cutting steps. In this case, the geological and stress conditions do not change. In the whole entry system, the pillar width is an important factor that affects the roof stress. But, in this study, the pillar width is fixed, 80 ft by 100 ft.

Table 3-1 Geological Conditions in Some Roof Failure Areas
(from some of the references [1]~[40])

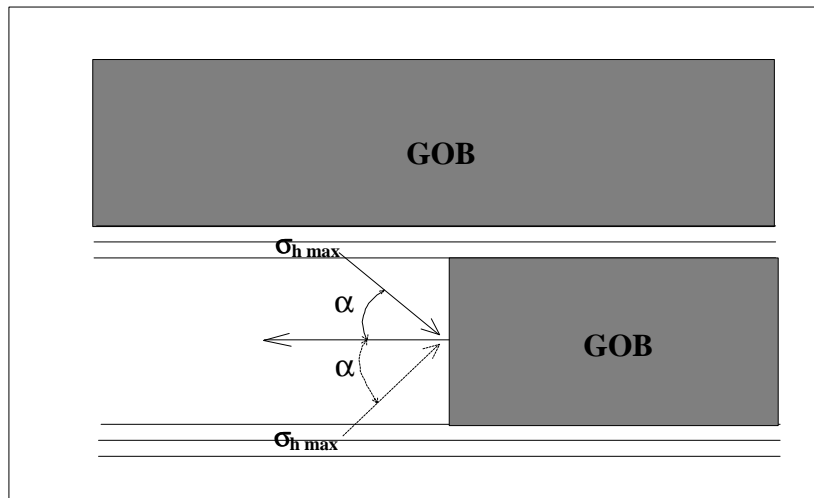
Mine	Coal Seam	Floor	Immed. Roof	Main Roof	Overburden (ft)	Remark
Greenwich	Lower Freeport	Limey underclay	10~16 ft dark gray shale	Sandy shale	665	R-and-P mining 18ft-entry
Springvale	Lithgow(8.8')	Fine sandstine	3ft siltstone & sandstone	Coarse sandstone	720~1,300	Australia 4.8m entry
Mine A Mine B	Pitts. Seam		Coal+laminated shale		700	Longwall CMRR=30s
Mine C	Eagle seam		Bedding shale		1,000	Longwall CMRR=55
Mine D	Eagle seam		Bedding shale		300	Longwall CMRR=55
Mine E			Semimassive shale		1,000	Longwall CMRR=50
Mine F			Interbedded sandstone and shale		500~1,000	Longwall in Alabama CMRR=43
Mine G			Laminated black shale (5ft)	siltier	1,000	Longwall in Kentucky CMRR=38
Mine H			Laminated black shale		1,150	longwall in Kentucky
			6~8ft gray and black shale	sandstone	1,050	
Steel No.2	6	Fireclay, shale, siltstone	Dykersburg shale		960	Room-and-pillar
Beckley coalfield	3~10ft	Thin fossiliferous shale	Sandy shale, Laminated sandstone		830~1,140	
Illinois Coal mine	No. 5 (5.5~6 ft)		Gray shale		930	



(a) Entry Development



(b) Single Panel Mining



(c) Multiple Panel System

Fig. 3-2 Finite Element Models (Plan View)

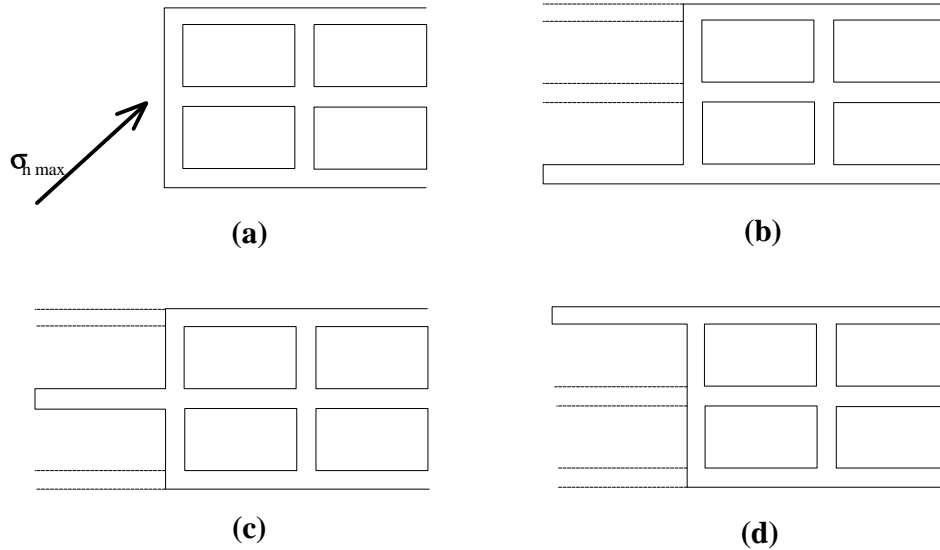


Fig. 3-3 Model of Sequence of Cutting in Entry Development

3.2.5 Influence of Interfaces between Layers

Generally, the laminated roof under the high horizontal stress may separate and slide between the layers. When roof separations and slip between the coal seam and the roof/floor occur, the roof stress will change. Over the years, some researchers have found that the stress in the roof may relieve to some degree when the slip occurs. However, since the interfaces between the coal and roof/floor and between the roof layers become discontinuous during the numerical analysis, many numerical softwares can not handle them. Therefore, research results about the roof separation and slip have been rarely reported.

In this study, the roof stress (plane strain) will be analyzed when the interfaces between the coal seam and the roof/floor and between the roof layers are involved. Assume that the cohesion in these interfaces is zero. The coefficient of friction ranges from 0.1 to 0.8. In addition, the vertical stress is fixed (the overburden depth in the models is 800 ft). The stress ratio of the applied horizontal stress to the vertical stress is 3, 4, 5, 6, and 7. The thickness of each roof layer is 1 ft.

3.2.6 Others

Gob characteristics is an important factor which affects the degree of stress relief around it. Gob size, shape, and compactness will influence the horizontal stress

distribution. But since there is not much information about the gob properties, the influence of the gob on the roof stress is not considered in this study.

Chain pillar is another factor that affects the roof stability in longwall mining, especially the tailgate entries. In this study, yield pillars are not taken into account. The width of chain pillar is fixed.

In this study, the influences of the above five factors on the stress distributions in the immediate roof of longwall entries are analyzed.

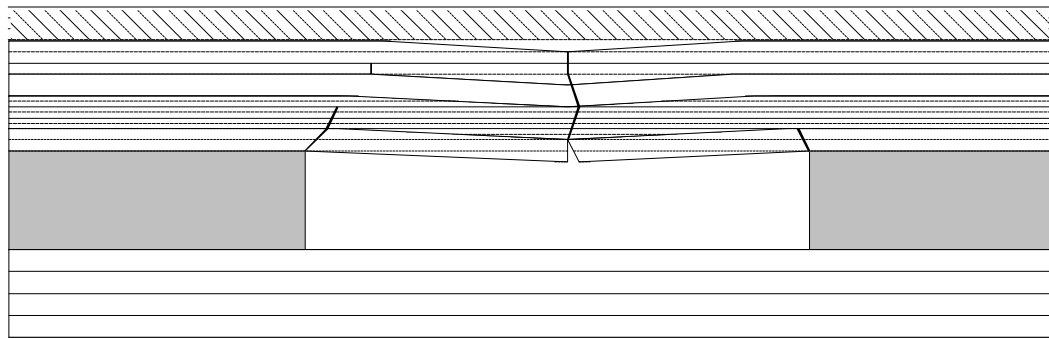
3.3 Selection of the Method of Analysis

As the emergence of high-speed and large-storage-capacity computer technology has widely used, the numerical stress analysis methods are being adopted in many areas of modern engineering. Three methods, especially, i.e., finite-element, finite-difference, and boundary-element methods, have become the most powerful tools of the design engineers and researchers. Among these three methods, the finite-element and boundary-element techniques are widely applied to the geomechanical problems. In this study, the finite element method is used. The finite element analysis softwares, ALGOR and ABAQUS, are used.

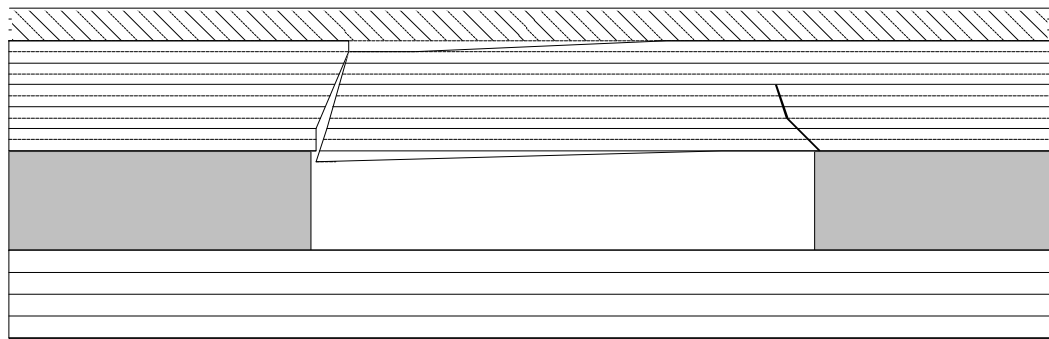
3.4 Mechanics of Roof Failure

3.4.1 Roof Failure Forms

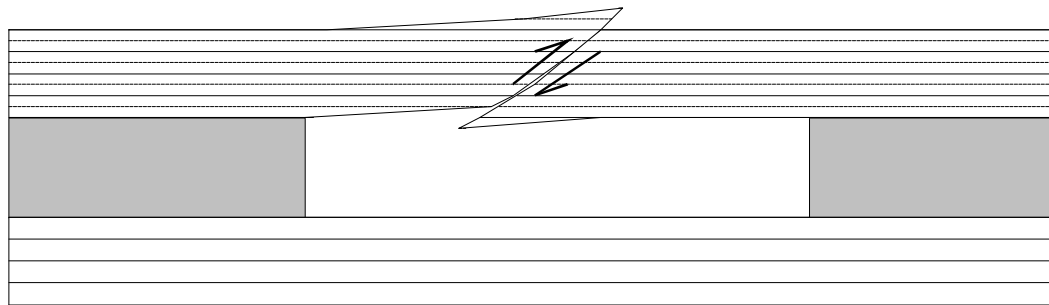
Underground observations have confirmed that there are two common types of roof failure, namely tensile failure and shear failure, as shown in Fig. 3-4. The mechanics of tensile failure of roof rock is considered in a rock beam with clamped edges. The beam fails in the middle under load at critical tensile strength. When a horizontal force acts on the beam, the roof span should be in compression. But, if the roof span is large, the midspan may be in tension.



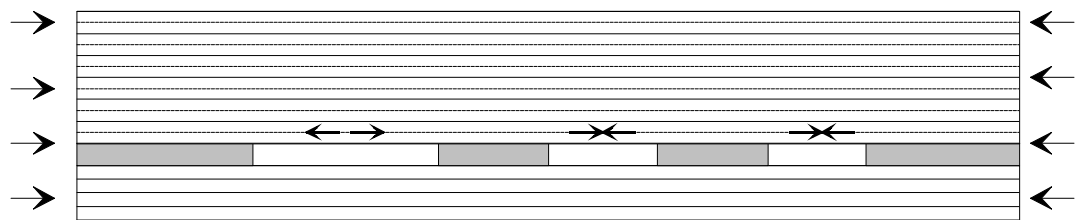
(a) Tensile Failure



(b) Shear Failure 1



(c) Shear Failure 2



(d) Roof in Different States Due to Different Spans

Fig. 3-4 Possible Forms of Roof Failure^[22]

Shear failure is most common for soft rock. When a horizontal stress exists, it develops just at the rib edges. Under a high horizontal stress, rock beam may buckle at midspan. This case usually occurs in strong strata.

The mechanical model of roof failure is shown in Fig. 3-5. The roof beam is subjected to a vertical load (p_v) and a horizontal stress (σ_{max}). In this model, the following parameters should be determined correctly, in order to have an analytical solution:

- a. the beam size, thickness w , and length L ;
- b. the vertical load distribution and the horizontal stress; and
- c. the end support methods of the beam

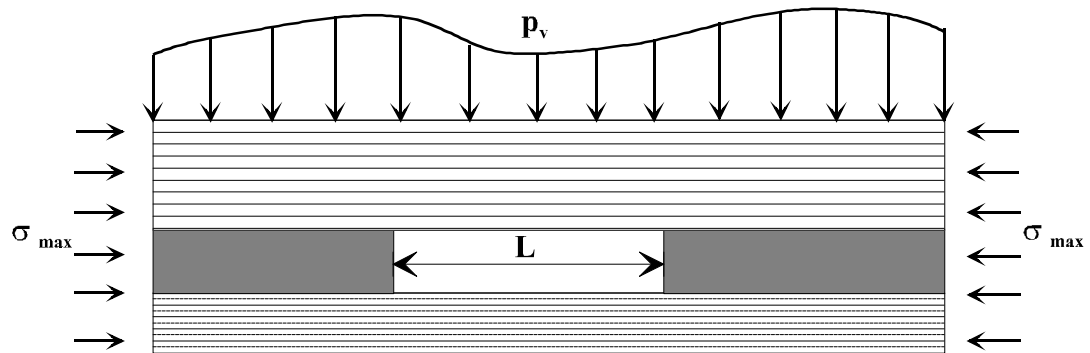


Fig. 3-5 Mechanical Model for Roof Failure

Usually, the immediate roof thickness can be considered as the beam thickness. But it is not easy to determine the vertical load distribution and the end support methods of the beam in underground conditions. Because the gob and the front abutment pressure of mining face will affect the vertical load distribution and immediate roof is neither a fixed beam nor a simply supported beam. In addition, an immediate roof generally consists of several layers of different strata, as shown in Fig. 3-6. In this situation, sliding will occur between the layers because of the different mechanical properties of the strata. In addition, if the horizontal stress is not perpendicular to the entry axis, the roof beam will be in a complicated stress field. Therefore, this model can hardly have an analytical solution. The only method to solve it is to use a numerical method, such as the finite element method. In this study, the finite element method will be used.

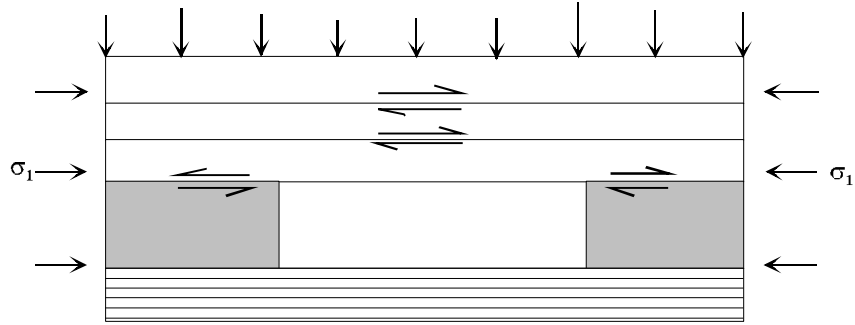


Fig. 3-6 Sliding Between Layers under Lateral Stress

If an immediate roof is a layer of rock and the vertical load is much smaller than the horizontal stress (Fig. 3-7), the critical horizontal stress (σ_{hc}) for a unit width beam can be determined by Euler's equation

$$s_{hc} = \frac{P^2 w^2 E}{12(IL)^2}$$

where w - the thickness of rock beam;

L - the length of the rock beam;

E - Young's modulus of beam; and

I - factor based on end support method

$I = 0.5$ for a fixed-end beam

$I = 0.7$ for a fixed-one-end, simple-supported-one-end beam

$I = 1.0$ for a simple-supported-end beam

$I = 2.0$ for a fixed-one-end, one-end-free beam

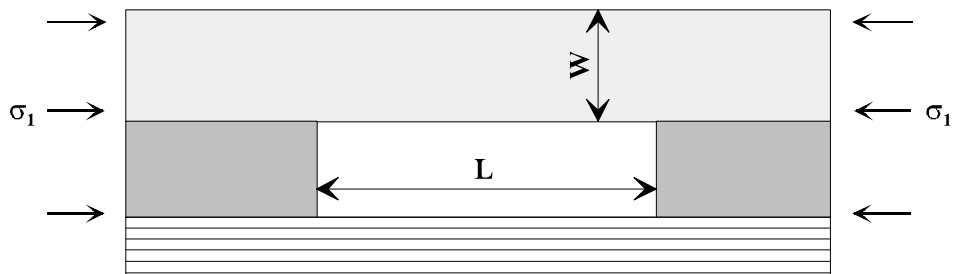


Fig. 3-7 Strong Roof Under High Horizontal Stress

When a horizontal stress $\sigma_{h \max}$ is equal to or larger than the critical stress σ_{hc} , the beam will buckle or yield. But, this equation is true only if the beam deformation follows the Hooke's law. If there exists a larger vertical loading, the beam fails more easily.

3.4.2 Roof Failure Criteria

To evaluate the roof stability, the key is to use a suitable rock failure criterion. As mentioned above, the roof failure may be caused either by a shear stress or by a tensile stress. So, different failure criteria should be used in different stress situations. In the following, some failure criteria have been introduced briefly.

Maximum Stress Criterion

This theory assumes that failure occurs when one of the principal stresses becomes equal to the failure stress in simple tension or compression. Since a rock material has very low tensile strength, it is thought that the rock material will fail when the minimum principal stress is equal to its tensile strength.

Von-Mises Stress Criterion

This theory assumes that failure begins in the material when the distortion energy equals to the distortion energy at failure in simple tension or compression. It can be expressed by the following equation:

$$\sqrt{\frac{(\mathbf{s}_1 - \mathbf{s}_2)^2 + (\mathbf{s}_2 - \mathbf{s}_3)^2 + (\mathbf{s}_3 - \mathbf{s}_1)^2}{2}} = \mathbf{s}_0$$

where $\mathbf{s}_1, \mathbf{s}_2, \mathbf{s}_3$ - principal stresses;

\mathbf{s}_0 - material strength obtained in testing

The Von-Mises stress (\mathbf{s}_{VM}) is defined by

$$\mathbf{s}_{VM} = \sqrt{\frac{(\mathbf{s}_1 - \mathbf{s}_2)^2 + (\mathbf{s}_2 - \mathbf{s}_3)^2 + (\mathbf{s}_3 - \mathbf{s}_1)^2}{2}}$$

Therefore, the Von Mises stress criterion becomes

$$\mathbf{s}_{VM} = \mathbf{s}_0$$

In a simple compressive test, the tested strength of material \mathbf{s}_0 is equal to the uniaxial compressive strength \mathbf{s}_c . In this case, this criterion is

$$\mathbf{s}_{VM} = \mathbf{s}_c$$

In a simple tensile test, the tested strength of material \mathbf{s}_0 is equal to the uniaxial tensile strength \mathbf{s}_t . In this case, this criterion is

$$\mathbf{s}_{VM} = \mathbf{s}_c$$

Considering the tensile and compressive strengths of material, a modified Von-Mises stress criterion^[14] (Pariseau, 1972; Dahl, 1972) is expressed by

$$\mathbf{s}_{VM} = \frac{\mathbf{s}_c - \mathbf{s}_t}{\mathbf{s}_c + \mathbf{s}_t} (\mathbf{s}_1 + \mathbf{s}_2 + \mathbf{s}_3) + 2 \frac{\mathbf{s}_c \times \mathbf{s}_t}{\mathbf{s}_c + \mathbf{s}_t}$$

Mohr-Coulomb Shear Critetion

This theory assumes that the material will fail when the shear stress on some plane reaches a value which depends on the normal stress acting on the plane. It can be defined by

$$\mathbf{t} = C + \mathbf{s}_n \tan(45^\circ + \frac{\mathbf{b}}{2})$$

where \mathbf{t} – shear stress on the plane;

C – cohesion of the material;

\mathbf{s}_n – normal stress on the same plane; and

\mathbf{b} – internal friction angle of the material

This criterion can also be expressed by the maximum and minimum principal stresses and the compressive strength of the material.

$$\mathbf{s}_1 = \mathbf{s}_c + \mathbf{s}_3 \tan^2\left(45^\circ + \frac{\mathbf{b}}{2}\right)$$

Maximum Shearing Stress Criterion

This theory assumes that failure occurs when the maximum shearing stress becomes equal to the shear strength of material.

$$\mathbf{t}_{\max} = \frac{\mathbf{s}_1 - \mathbf{s}_3}{2}$$

Since each failure criterion has its own limitation of application and the rock strength depends on the stress conditions (for example, the rock strength is different in uniaxial tests from in triaxial tests), it is difficult to tell which criterion is better. The selection of the rock failure criterion must be based on the underground observations and the rock lab tests. Therefore, this study does not deal with the failure criteria and only the stresses, such as the Von-Mises stress, the maximum and the minimum principal stresses, in the entry roof are analyzed.

3.5 Initial Study

During a modeling analysis, five factors, i.e., overburden depth, horizontal stress, roof type, angle, and ratio, must be taken into account. In the overburden, there are three levels, 500 ft, 800 ft, and 1,300 ft. The maximum horizontal stress is 3,000 psi and 4,500 psi, respectively. In addition, weak and medium strength roofs should be considered. Since the angle between the orientation of the maximum horizontal stress and mining/entry development direction ranges from 15° to 90°, increasing per 15° and the

ratio of the maximum to minimum horizontal stresses is 1.2, 1.5, and 2.0, respectively, there are totally 216 combinations, as shown in Fig. 3-8. If all the combinations are considered in the study of stress distributions of immediate roof in entry development, single longwall panel, and multiple longwall panels, it will take very long time. Moreover, it is not necessary. The primary objective of this initial study is to determine the ranges of influence of these factors and to reduce the unnecessary work.

3.5.1 Problem Definition and Conditions

The initial study simulates a single entry in all combinations. A model is shown in Fig. 3-9. The entry is 18 ft wide and 100 ft long. The model is about 400 ft wide and 400 ft long. The simulated roof height is 50 ft. The coal seam is 7 ft thick. The floor thickness is 30 ft. The number of the element is about 10,000. The minimum size of the elements in the area of interest is 3x5x5 ft. The stresses along lines L1~L5 will be analyzed. The lines L1~L5 are at the roof line level. Lines L1 and L5 are respectively located at the upper corners of the entry. Line L3 is at the center of the roof. Lines L2 and L4 are near line L1 and L5, respectively. The distance from L2 to L1 (also from L4 to L5) is 1.5 ft. The maximum horizontal stress is from the side of line L1, as shown in Fig. 3-9.

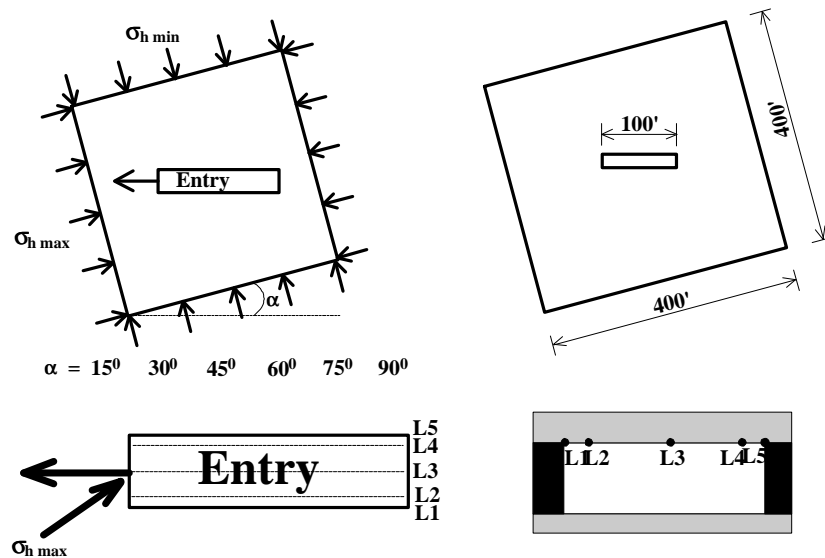
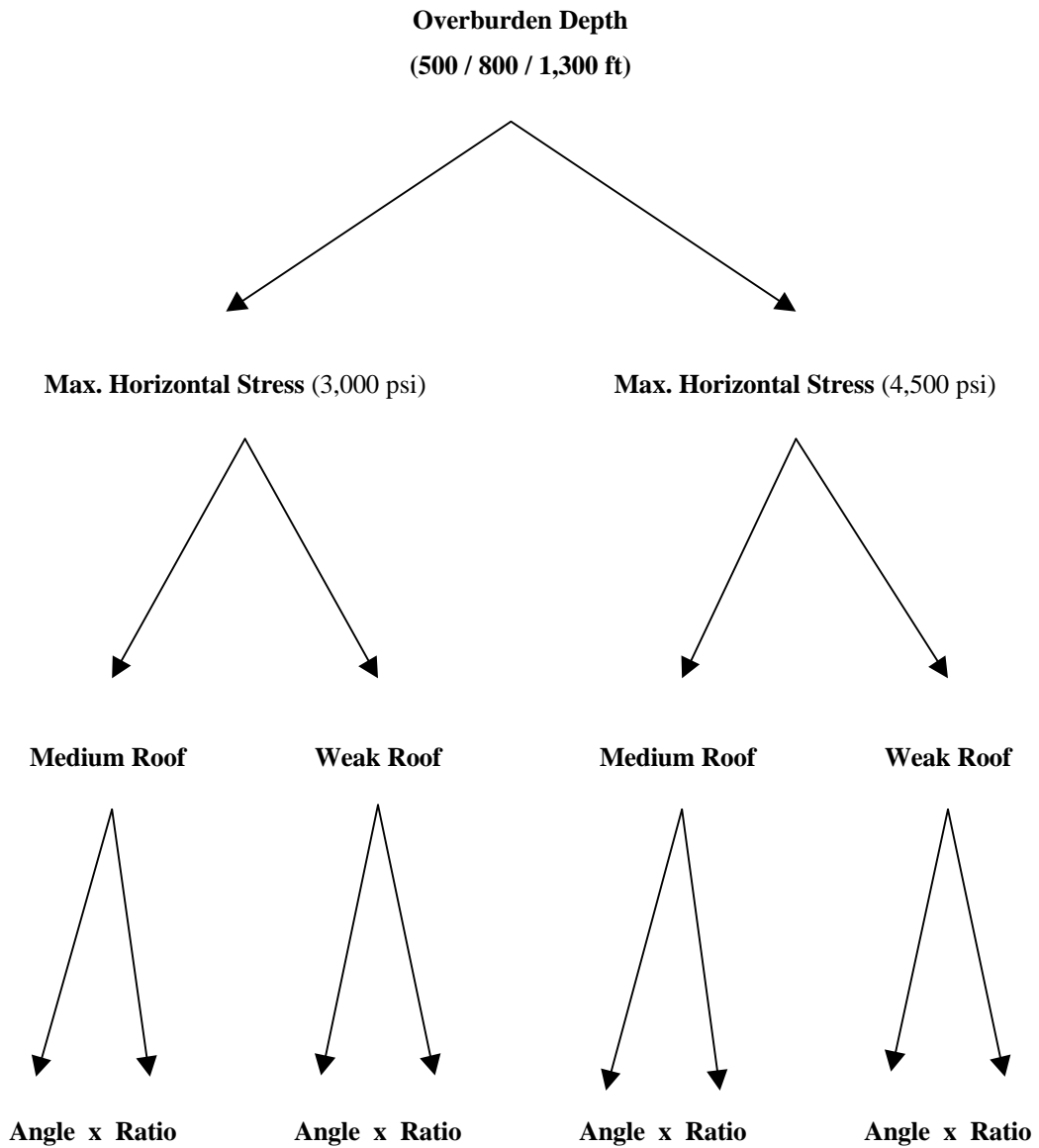


Fig. 3-9 Plan View of 3-D Models for Initial Study and Location of Measurement Lines



Angle (α) = 15° , 30° , 45° , 60° , 75° , and 90° Ratio = $\sigma_{hmax} / \sigma_{hmin} = 1.2, 1.5, \text{ and } 2.0$

σ_{hmax} , σ_{hmin} - maximum and minimum horizontal stresses

There are totally 216 combinations.

Fig. 3-8 Combinations of Main Factors Considered in the Study

The rock mechanical properties are listed in Fig. 3-1. The assumptions regarding the material properties are the following:

- a. the material or rock types which make up the model are isotropic, homogeneous, and continuous within each layer, and
- b. they demonstrate a linear elastic behavior.

3.5.2 Analysis and Discussion of Results

In order to evaluate the effects of horizontal stress on entry roof, first the stress in the immediate roof is analyzed when an entry is only subjected to the gravitation (without horizontal stress). Then, the stress distributions in the entry roof are studied when the entry is under high horizontal stress. Through the comparison of the stress difference between these two cases, the horizontal effects can be evaluated.

Stress Distributions without Horizontal Stress

Fig. 3-10 shows the stresses in the immediate roof when the overburden depth is 1,300 ft. In this figure, a positive value denotes compressive stress while a negative one is for tensile stress. In Fig. 3-10, the stresses along five lines, numbered L1~L5, are presented. The locations of these five lines are shown in the figures. Line L3 is in the center of entry roof, while line L1 and L5 are in the two sides of the entry roof. Lines L2 and L4 are near L1 and L5, respectively. Fig. 3-10 indicates that the stress distributes symmetrically in the immediate roof and that the stress distributions have the following patterns:

- a. the Von-Mises stresses in the two sides of the entry roof (L1 and L5) are larger than those along the other lines, while in the center of entry roof the stress is the minimum (Fig. 3-10(a));
- b. the minimum principal stress in the center (along L3) reaches the minimum (namely, the maximum tensile stress occurs in the entry center), as shown in Fig. 3-10 (b);
- c. the maximum principal stress reaches the maximum at the two sides of entry roof and the minimum at the entry center (Fig. 3-10(c));

- d. the influence of roof properties on the patterns of stress distributions is small. Either in the medium strength roof or in the weak roof, the stress distributes in the same way (compared Fig. 3-10 (d)~(f) with (a)~(c)).

In the different overburden depth, the magnitude of stress is different. But the pattern of stress distribution is the same. Based on the above analysis, it is found that the shear failure may occur in the two sides of entry roof while the tension failure may happen in the entry center without high horizontal stress.

Stress Distributions with Horizontal Stress

When an entry is subjected to a high horizontal stress, the stress distributes in a different way. Fig. 3-11 shows the stress distributions in the weak immediate roof. In this case, the overburden depth is 1,300 ft, the maximum horizontal stress is 4,500 psi, the ratio of the maximum to minimum horizontal stresses is 2.0, and the angle between the entry development direction and the maximum horizontal stress is 60° . It shows:

- a. the stress distribution is not symmetric in high horizontal stress field. The stress in one side of entry roof is larger than that in the other, which indicates that the stress in one side relieves to some degree;
- b. the Von-Mises stress in one side of entry roof (along line L4) is the largest. In the center of the entry, the Von-Mises stress is the minimum (along L3);
- c. the minimum principal stress in the center of entry roof is larger than those along lines L2 and L3. The maximum tensile stress occurs where the Von-Mises stress reaches the maximum along each line;
- d. the pattern of the maximum principal stress distribution is the same as that without horizontal stress. In the entry center, it is the minimum while in the two sides it is larger.
- e. Compared with Fig. 3-10, it is found that the stress in this case is larger. For example, without horizontal stress, the maximum Von-Mises stress is about 1800 psi, while it is about 3,000 psi with horizontal stress. The minimum principal stress also increases. In the first case, it is about -800 psi (tensile stress). In the second case, it is about -300 psi. The maximum principal stress

increases, too. This indicates that the possibility of shear failure in the immediate roof is larger with horizontal stress than that without horizontal stress. But, the possibility of tension failure reduces under horizontal stress.

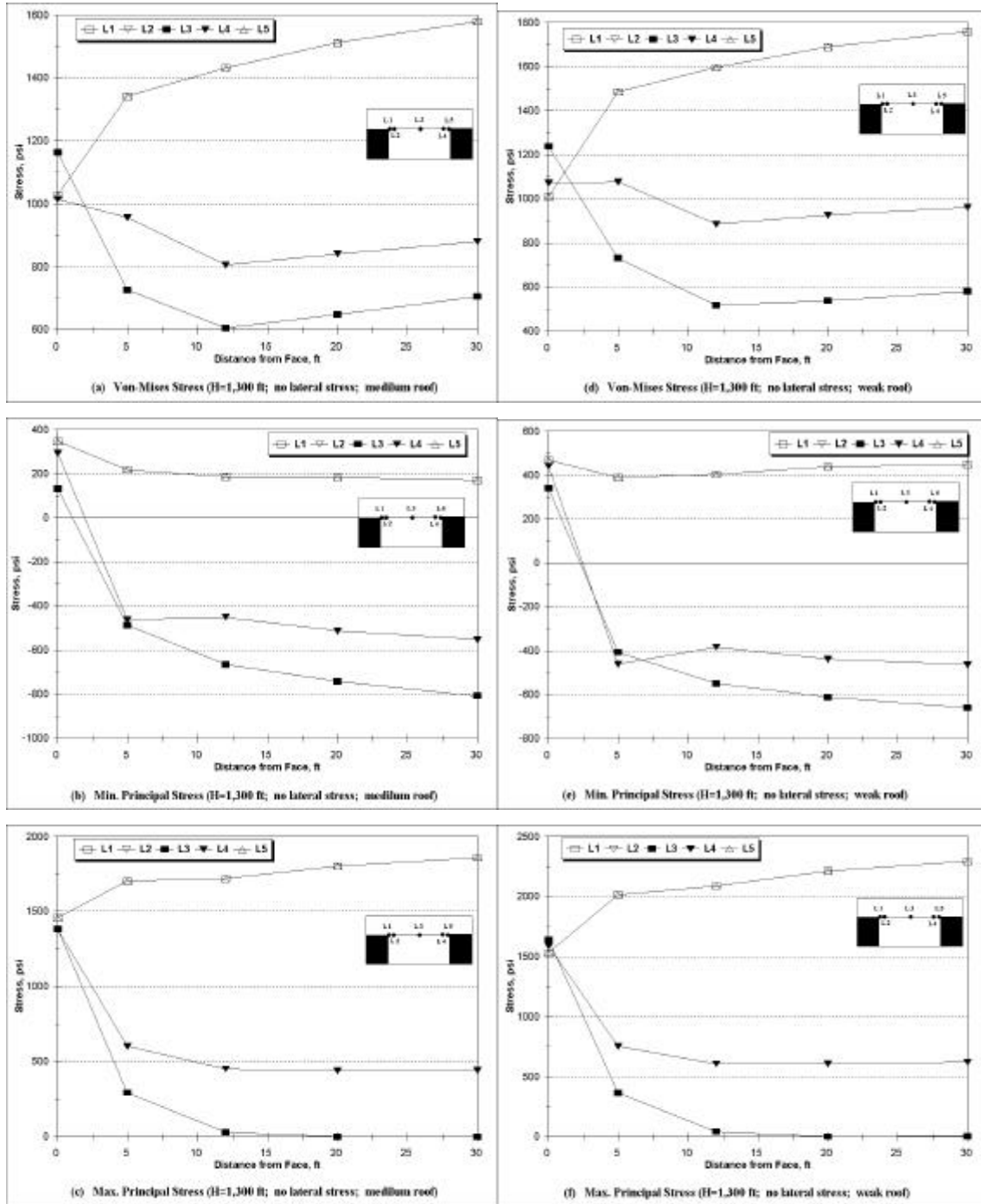


Fig. 3-10 Stress Distributions in Immediate Roof without Horizontal Stress

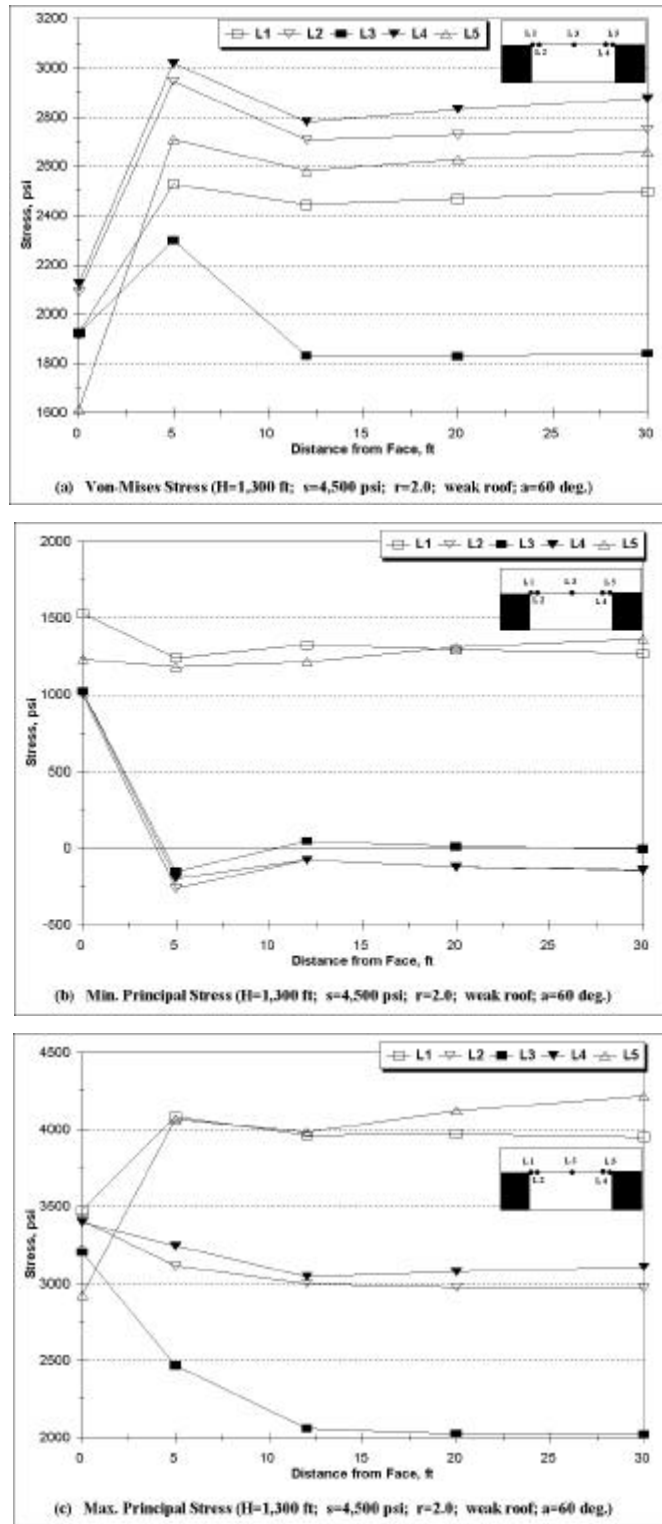


Fig. 3-11 Stress Distributions in Immediate Roof with Horizontal Stress

The above analysis indicates that the horizontal stress does have a significant influence on stress distributions in the immediate roof. It changes the patterns of stress and the location of roof failure. Since a larger tensile stress and a larger Von-Mises stress occur near the pillar ribs, cutter roof failure may often happen.

All the combinations confirm that the Von-Mises stress and the tensile stress at the point that is located in line L4 and near the entry face are the largest. Therefore, the stress change at this point in the different cases will be discussed in the following.

Tables 3-2 and 3-3 summarize the Mises stress and the minimum principal stress at the point where the maximum stress occurs in all models (all combinations). Figs. 13~15 show the Von-Mises stress and the minimum principal stress changes in the different conditions. From these tables and figures, the effect of each factor can be found.

Angle Effect

The angle between the orientation of the maximum horizontal stress and the entry development direction is an important factor that affects the entry roof. Table 2 indicates that the Von-Mises stress increases significantly with the angle no matter what type of roof and stress conditions. Fig. 3-12 shows the Von-Mises stress change with the angle when the overburden depth is 800 ft and the maximum horizontal stress is 4,500 psi. When the ratio of the maximum to minimum horizontal stresses ranges from 1.2 to 2.0, the stress increases with the angle in the weak and medium roofs. When the angle is equal to or larger than 45° , the stress increases significantly. When the angle is 90° , the stress reaches the maximum. For a single entry, in this case, the stress in the immediate roof distributes symmetrically.

The minimum principal stress also changes with the angle. As shown in Table 3-3, the tensile stress reaches the maximum when the angle is about 60° . However, the angle influence on the tensile stress is not as significant as that on the Von-Mises stress.

Overburden Depth

Fig. 3-13 shows the influence of overburden depth on the stress distributions. In the weak roof, when the maximum horizontal stress is 3,000 psi, the Von-Mises stress increases slightly with the overburden depth, as shown in Fig. 3-13(a). The increment of the Von-Mises stress is under 10%. For example, when the angle is 60°, the stress at the overburden depth of 500 ft is about 1,900 psi. While it is about 2,050 psi when the overburden depth is 1,300. When the maximum horizontal stress is 4,500 psi, the trend is the same. The Von-Mises stress slightly increases with the overburden depth, as shown in Fig. 3-13(c). In the medium roof, the Von-Mises stress slightly reduces with the overburden depth, as shown in Fig. 3-13(b) and (d). Fig. 3-13 indicates that the influence of the overburden depth on the Von-Mises stress in the immediate roof is very small. From the Von-Mises stress point of view, the overburden effect on the entry roof can be ignored.

However, the overburden has a significant influence on the minimum principal stress in the immediate roof, as shown in Fig. 3-14. It indicates that the tensile stress increases with the overburden depth. At larger depths, the tensile stress is larger when the horizontal stress keeps constant.

Ratio of Horizontal Stresses

The ratio of the maximum to the minimum horizontal stresses has an effect on the stress distributions in the immediate roof. Like the overburden depth, the stress increases slightly with the decrease of the ratio, as shown in Tables 3-2 and 3-3. Fig. 3-15 shows the Von-Mises stress change in the weak roof with the ratio for different horizontal stress when the overburden depth is 1,300 ft. It is found that the Von-Mises stress increases slightly when the ratio reduces. When the ratio ranges from 2.0 to 1.2, the Von-Mises stress adds about 5~10%. As shown in Table 3-3, the ratio influence on the minimum principal is very small and can be ignored.

Generally, the ratio effects on the entry roof can be ignored.

Roof Properties

In this study, two types of roof are considered, weak roof and medium roof, because roof failure often occurs in these types of roof. It is found by the finite element analysis that the pattern of stress distributions in the immediate roof does not change with the roof type, but the magnitude of the stress changes. In the weak roof (with small Young's modulus) the Von-Mises stress is smaller than that in the medium roof (with large Young's modulus), as shown in Fig. 3-16.

3.5.3 Summary

Based on the above stress analysis, the effects of the factors which may influence the stress distributions in the immediate roof of longwall entries have the following characteristics:

- a. The stress distribution in the immediate roof of entry under high horizontal differs from that without horizontal stress. In this case, the Von-Mises and tensile stresses at one side of the roof are larger than those at the other side. In addition, usually the maximum tensile stress does not occur in the center of entry, it occurs at the same point where the maximum Von-Mises stress appears.
- b. The angle between the orientation of the maximum horizontal stress and the entry development direction is an important factor. When the angle is equal to or larger than 45° , its effect is significant. The Von-Mises stress increases with the angle from 0° to 90° . Generally, it increases slowly from 0° to 45° , and then rapidly from 45° to 90° . In addition, the stress along line L5 is larger than that along line L1 when the maximum horizontal stress is from the L1 side. Comparing Fig. 3-12 and Fig. 2-18, it is found that the Von-Mises stress distributions accord with the distributions of roof shear failures.
- c. The ratio of the maximum to the minimum horizontal stress has an effect on the Von-Mises stress in the roof. But this effect is not significant, although the Von-Mises stress increases as the ratio decreases.

- d. The influence of the overburden depth on the Von-Mises stress in the roof is not significant under high horizontal stress. However, the tensile stress in the immediate roof increases with the overburden depth significantly.
- e. The roof type affects the magnitude of stress, but does not change the pattern of stress distribution. The Von-Mises stress in the medium roof is larger than that in the weak roof. But the tensile stress in the weak roof is larger than that in the medium roof.

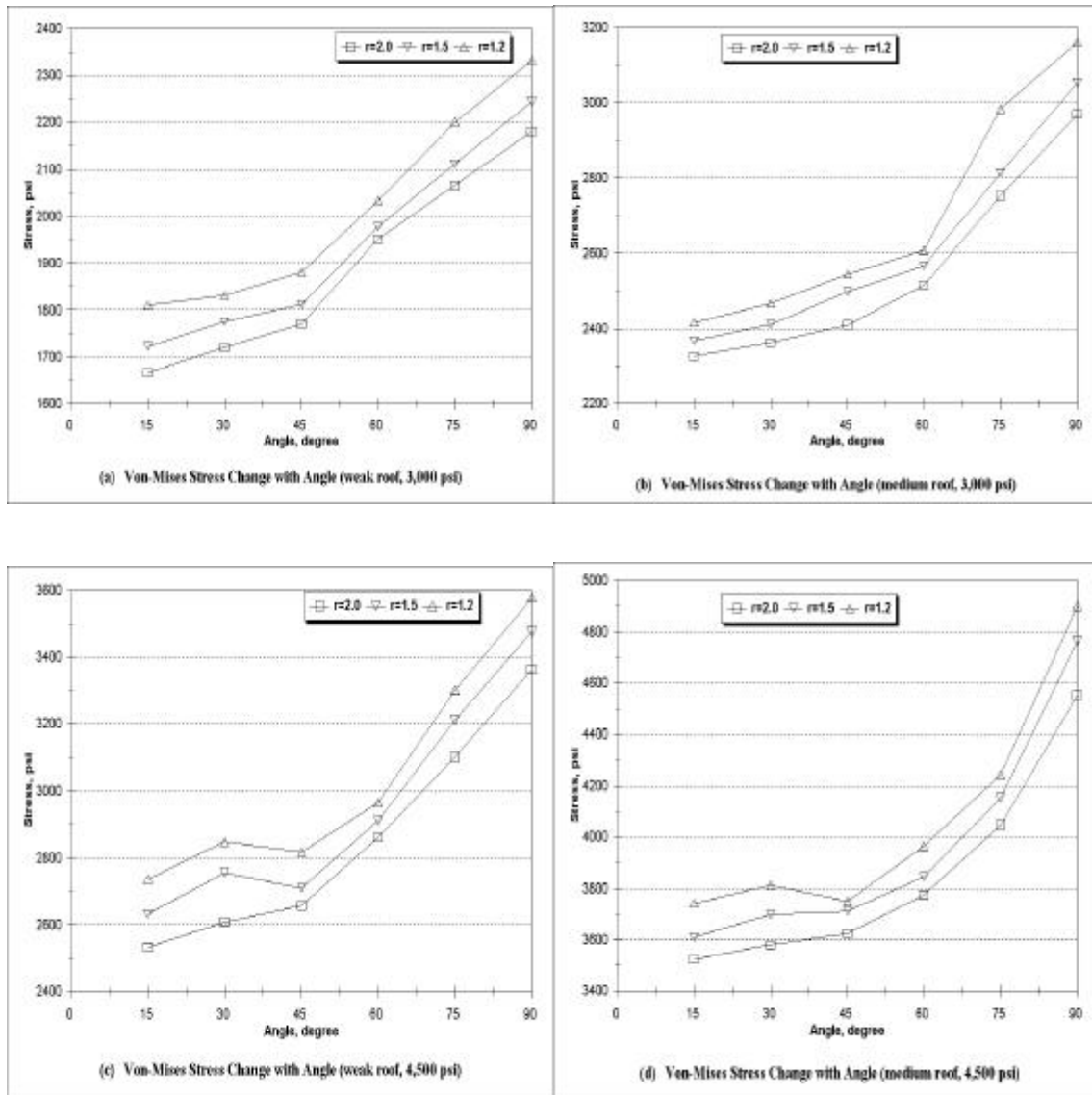


Fig. 3-12 Von-Mises Stress Changes in Immediate Roof with the Angle

**Table 3-2 Von-Mises Stresses at the Point where the Maximum stress occurs
under Various Combinations of the Main Factors**

Max. H. Stress (psi)	Roof Type	Angle α ($^{\circ}$)	Overburden Depth (ft)								
			500			800			1,300		
			Ratio			Ratio			Ratio		
			2.0	1.5	1.2	2.0	1.5	1.2	2.0	1.5	1.2
3,000	medium	15	2430	2443	2454	2327	2368	2417	2286	2351	2396
		30	2466	2487	2504	2363	2412	2467	2322	2401	2446
		45	2514	2556	2581	2411	2498	2544	2370	2413	2523
		60	2618	2632	2645	2515	2567	2608	2474	2511	2587
		75	2857	2899	3022	2754	2815	2985	2713	2856	2964
		90	3073	3112	3198	2970	3054	3161	2929	3034	3140
	Weak	15	1619	1711	1749	1667	1723	1811	1773	1812	1882
		30	1672	1723	1769	1720	1776	1831	1826	1878	1935
		45	1723	1781	1819	1771	1812	1881	1877	1923	1986
		60	1903	1945	1972	1951	1978	2034	2057	2098	2166
		75	2018	2105	2139	2066	2112	2201	2172	2213	2281
		90	2133	2211	2270	2181	2245	2332	2287	2321	2396
4,500	Medium	15	3589	3623	3798	3524	3611	3742	3443	3578	3677
		30	3647	3712	3869	3582	3698	3813	3501	3621	3748
		45	3690	3745	3806	3625	3711	3750	3544	3645	3685
		60	3840	3891	4021	3775	3845	3965	3694	3776	3900
		75	4113	4189	4299	4048	4154	4243	3967	4098	4178
		90	4620	4811	4957	4555	4765	4901	4474	4687	4836
	Weak	15	2505	2611	2689	2533	2634	2737	2616	2710	2851
		30	2581	2721	2801	2609	2756	2849	2692	2832	2963
		45	2630	2689	2770	2658	2710	2818	2741	2786	2932
		60	2833	2867	2917	2861	2912	2965	2944	2988	3079
		75	3073	3123	3252	3101	3213	3300	3184	3289	3414
		90	3335	3415	3529	3363	3476	3577	3446	3552	3691

**Table 3-3 Min. Principal Stresses at the Point where the Maximum stress occurs
under Various Combinations of the Main Factors**

Max. H. Stress (psi)	Roof Type	Angle α ($^{\circ}$)	Overburden Depth (ft)								
			500			800			1,300		
			Ratio			Ratio			Ratio		
			2.0	1.5	1.2	2.0	1.5	1.2	2.0	1.5	1.2
3,000	medium	15	-5	2	8	-62	-52	-44	-184	-167	-153
		30	-26	-22	-18	-86	-79	-74	-214	-198	-188
		45	-31	-27	-24	-93	-84	-79	-222	-204	-194
		60	-45	-34	-24	-112	-95	-81	-245	-219	-198
		75	-17	-6	4	-77	-62	-49	-202	-179	-159
		90	5	17	28	-48	-33	-20	-160	-138	-121
	Weak	15	-38	-34	-31	-116	-110	-105	-268	-257	-248
		30	-71	-70	-71	-153	-150	-148	-308	-300	-295
		45	-81	-80	-80	-163	-160	-159	-321	-311	-306
		60	-106	-93	-82	-192	-175	-161	-348	-327	-309
		75	-66	-52	-39	-148	-130	-115	-300	-278	-258
		90	-22	-13	0	-102	-84	-68	-248	-224	-204
4,500	Medium	15	32	40	48	-14	-5	5	-114	-98	-85
		30	4	8	12	-46	-40	-35	-151	-139	-131
		45	-5	0	4	-54	-48	-43	-160	-147	-138
		60	-20	-7	-5	-77	-59	-44	-192	-164	-142
		75	16	30	43	-34	-17	-1	-138	-113	-92
		90	45	60	75	1	18	35	-91	-68	-47
	Weak	15	1	5	9	-68	-61	-56	-202	-191	-183
		30	-45	-45	-47	-118	-117	-117	-258	-252	-250
		45	-59	-60	-61	-133	-131	-132	-272	-268	-265
		60	-93	-76	-61	-173	-152	-134	-318	-291	-269
		75	-37	-19	-3	-111	-89	-70	-250	-223	-198
		90	13	32	51	-52	-30	-9	-180	-152	-127

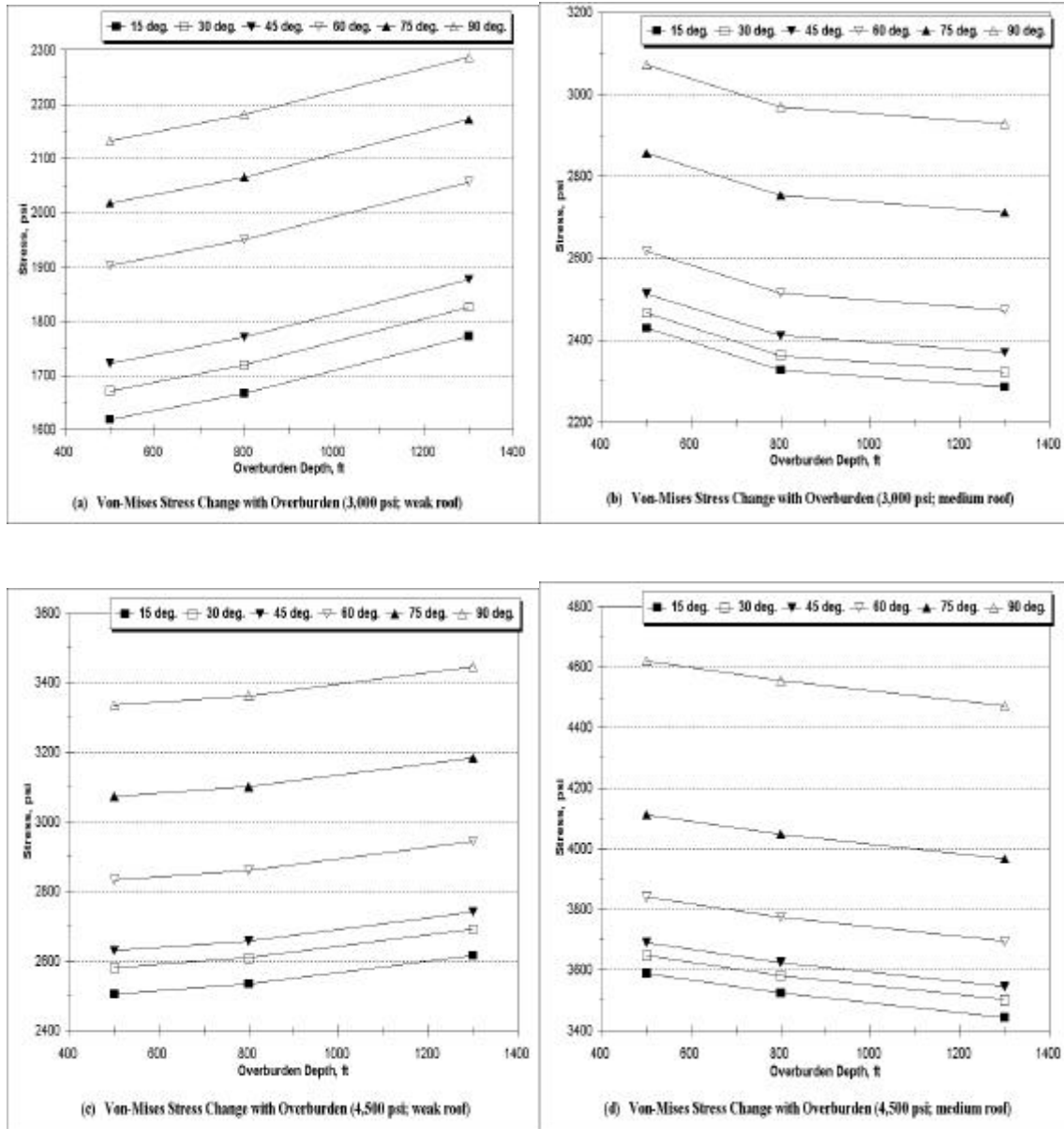


Fig. 3-13 Von-Mises Stress Distributions in Immediate Roof with Different Overburdens

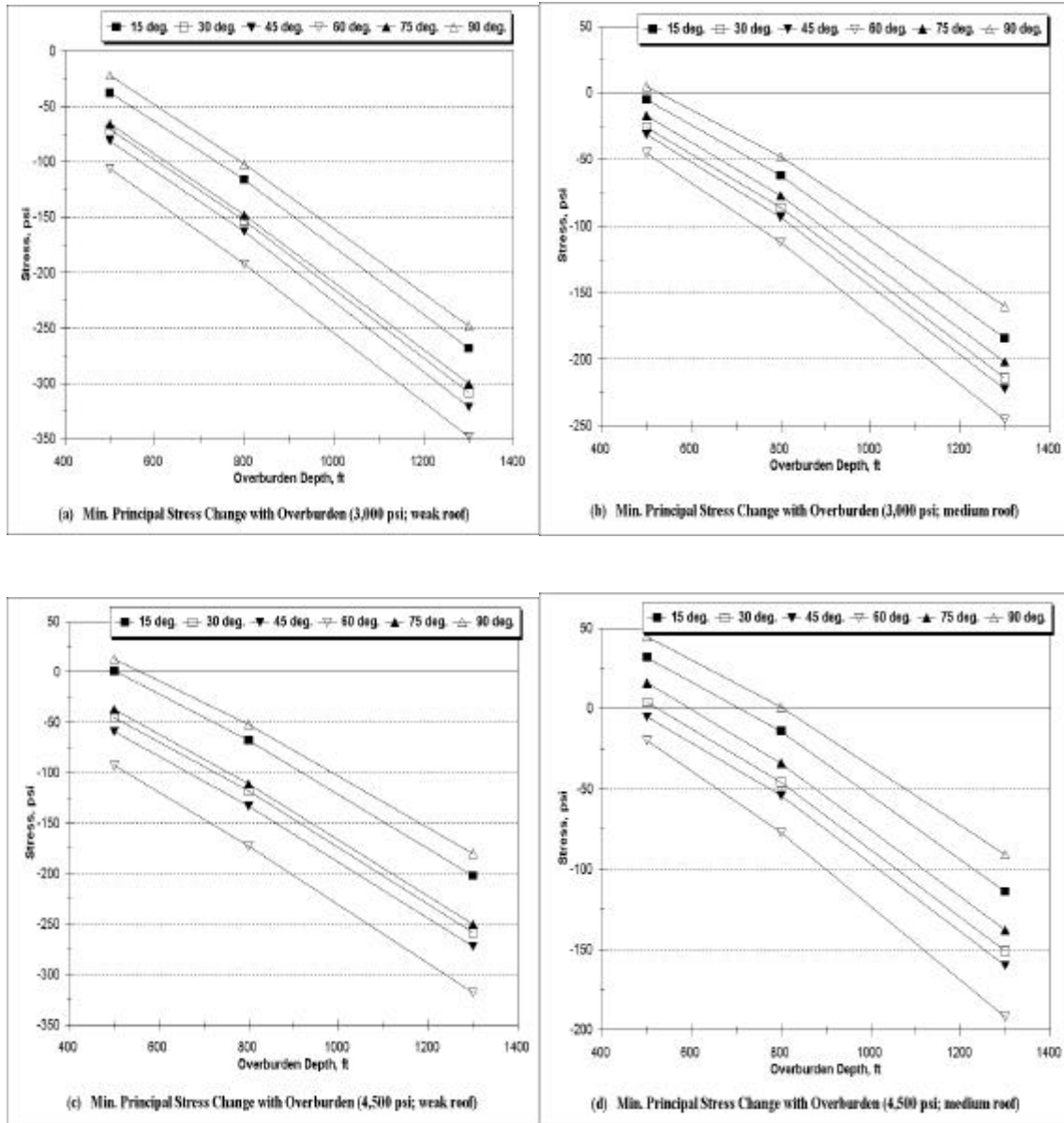


Fig. 3-14 Min. Principal Stress Distributions in Immediate Roof with Different Overburdens

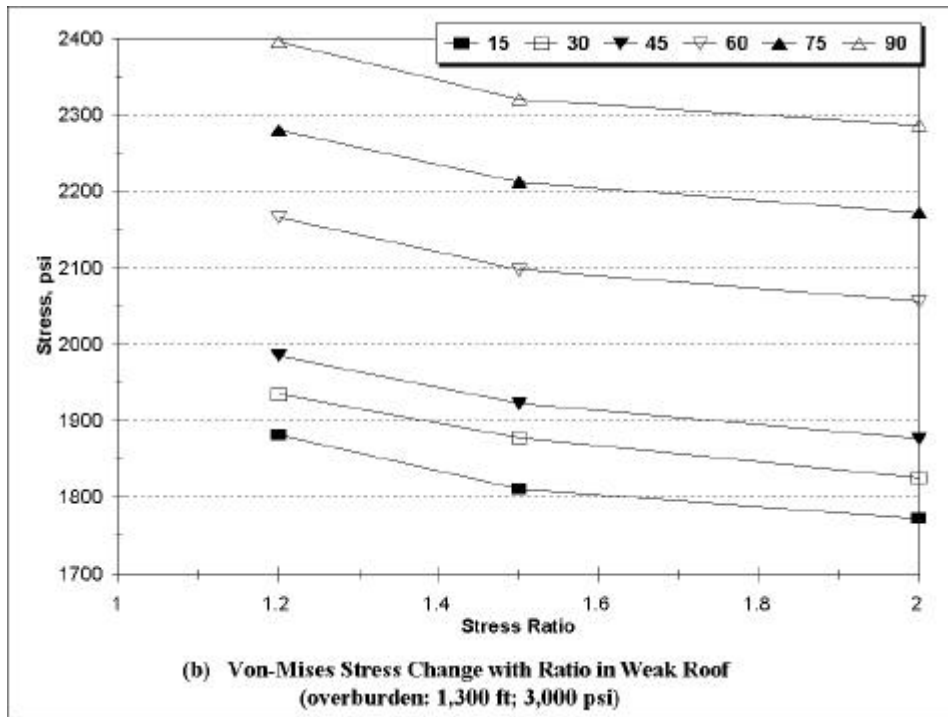
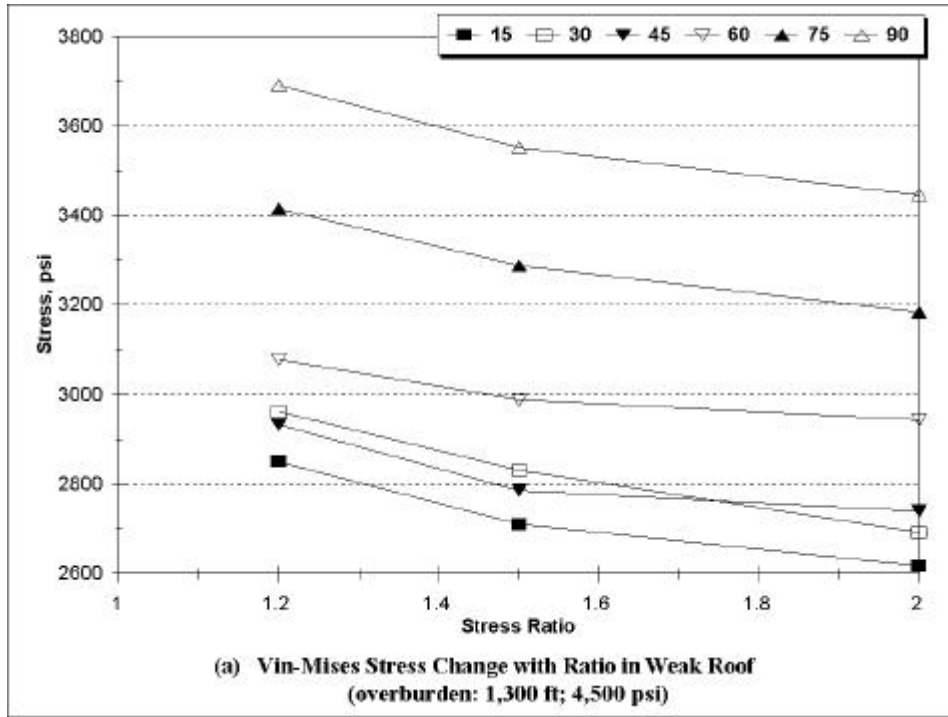


Fig. 3-15 Von-Mises Stress Changes with the Stress Ratio

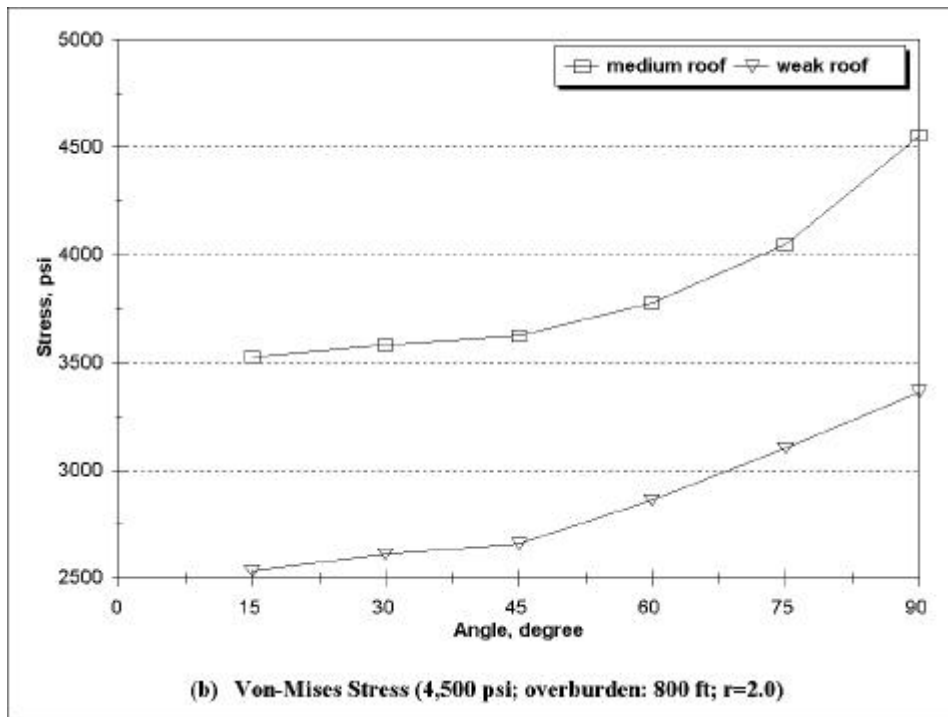
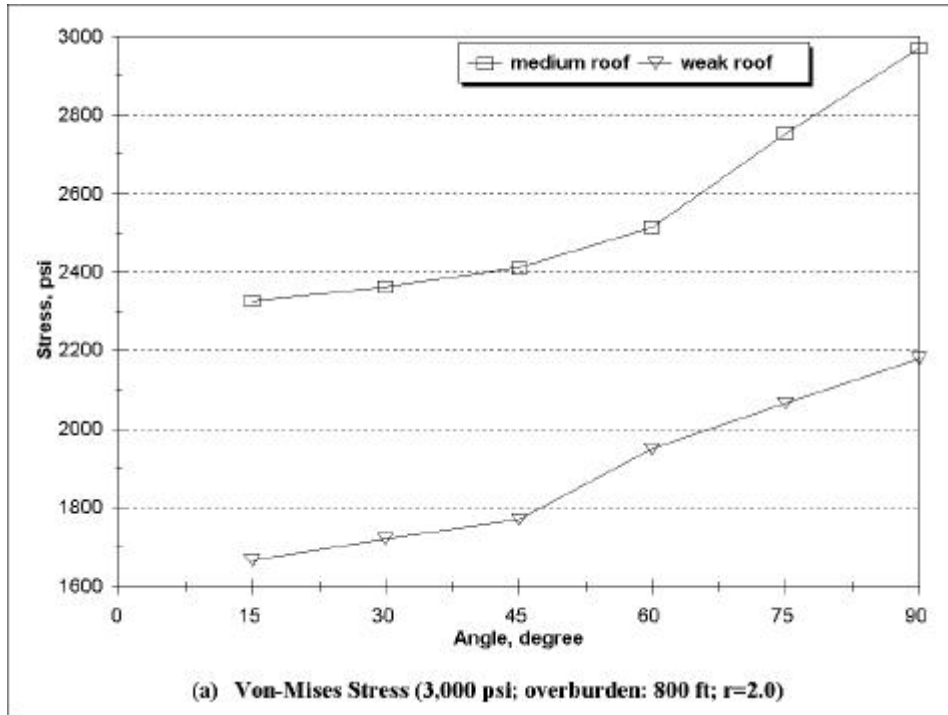


Fig. 3-16 Von-Mises Stress distributions in the Different Types of Immediate Roof